Low-Bandgap Conjugated Polymers. A Joint Experimental and Theoretical Study of the Structure of Polyisothianaphthene

I. Hoogmartens, P. Adriaensens, D. Vanderzande, and J. Gelan

Limburg University, Instituut voor Materiaalonderzoek (IMO), Departement SBG, Universitaire Campus, B-3590 Diepenbeek, Belgium

C. Quattrocchi, R. Lazzaroni,† and J. L. Brédas*

Service de Chimie des Matériaux Nouveaux, Département des Matériaux et Procédés, Université de Mons-Hainaut, 20 Place du Parc, B-7000 Mons, Belgium

Received May 28, 1992; Revised Manuscript Received September 23, 1992

ABSTRACT: We investigated the structure of a low-bandgap conjugated polymer, polyisothianaphthene (PITN), with a joint experimental and theoretical approach. On the one hand, ^{13}C NMR measurements are performed on the polymer and on a series of model isothianaphthene molecules. These molecular compounds are designed and synthesized to represent either aromatic or quinoid segments of the polymer chain. Combining cross-polarization magic angle spinning (CP/MAS), cross-depolarization (CDP), and proton-dephasing (PDP) experiments as a function of the polarization and the depolarization time allows determination of the chemical shifts of the four carbon of PITN. These values are compared to the data obtained on the model molecules and discussed in terms of the ground-state structure (aromatic or quinoid) of the polymer. On the other hand, quantum-chemical calculations using the Austin model 1 (AM1) semiempirical Hamiltonian are performed on ITN oligomers of various lengths. The relative stabilities of the aromatic and quinoid valence bond isomers are estimated in relation to the corresponding values for polythiophene. Finally, the electronic properties (bandgap, ionization potential) of aromatic and quinoid PITN are evaluated with the valence effective Hamiltonian method and compared to the experimental data.

1. Introduction

Conjugated polymers have attracted a broad interest over the past decade, in particular because in the doped state they represent a new class of light-weight electrically conductive materials.[1] In contrast, in the neutral state, most of these polymers are wide-bandgap semiconductors. However, the introduction of side groups to induce specific electronic interactions with the conjugated backbone opened the way to the design of low-bandgap systems with the ultimate goal of producing intrinsically conductive polymers. This synthetic approach was first considered by Wudl et al.,[2] who successfully reduced the bandgap of polythiophene by fusing a benzene ring into each thiophene unit. The so-obtained polyisothianaphthene (PITN) possesses a 1-eV bandgap, as determined from optical absorption, compared to 2 eV for the parent thiophene polymer.

Following this breakthrough, it was shown from quantum-chemical calculations that the bandgap of nondegenerate ground-state conjugated polymers, such as polythiophene, is directly related to the degree of bond-length alternation between the carbon–carbon single and double bonds along the backbone.[3] The valence bond structure of the polythiophene chain is considered to be aromatic-like; i.e., it is characterized by bonds between the α- and β-carbons of the thiophene ring markedly shorter (double-bond character) than the β–β' and inter-ring bonds (single-bond character). Therefore, chemical modifications stabilizing the quinoid valence bond isomer, which corresponds to a reversed single-bond–double-bond pattern, are likely to reduce the bond-length alternation and, hence, the bandgap. This mechanism has been shown to operate in several pyrrole and thiophene polymers, including PITN, giving rise to a series of low-bandgap systems.[4]

† Chercheur Qualifié du Fonds National de la Recherche Scientifique (Belgium).

The above-mentioned calculations also predicted that, for larger stabilizations of the quinoid form, the bandgap would rise again. In that case, the ground state of the polymer would correspond to a quinoid geometric structure, with a significant degree of bond-length alternation: inter-ring bonds and β–β' bonds would show a strong double-bond character. As a consequence, a polymer with a given bandgap may have either a quinoid or an aromatic geometric structure, depending on the relative stability of the two forms. While the ground-state geometric structure of most conjugated polymers built from aromatic molecules clearly remains aromatic, that question has not been resolved unequivocally yet in the case of PITN and has been the object of some controversy in the literature.

The first calculations of the electronic structure of PITN were performed on the aromatic form, in the basis of the geometry of the monomer. Those results correctly confirmed the 1-eV reduction of the bandgap when going from polythiophene to PITN.[5] Later, a modified neglect of diatomic overlap (MNDO) geometry optimization of the polymer chain indicated the quinoid form to be more stable, even though the dimer maintains a completely aromatic character.[6] (Note however that, in the case of polythiophene, the MNDO approach predicts the aromatic structure to be only 3.5 kcal/mol per repeat unit more stable than the quinoid form while with ab initio and other semiempirical methods, including those used in this work, this difference is at least twice as big.[7–9]) Recently, Nayak and Marynick,[8] using the partial retention of diatomic differential overlap (PRDDO), have found that the quinoid form of PITN is actually very slightly favored over the aromatic one (ΔE = 2.4 kcal/mol per repeat unit) whereas a simple Hückel study indicates that the aromatic character of short PITN oligomers gradually vanishes as the chain length increases.[10]

Besides the quantum-chemical calculations, the experimental evidence available up to now is not definitely conclusive. Because of the amorphous nature of most conjugated polymers, direct structural information ob-

0024-9297/92/2225-7347$03.00/0

tained from X-ray or neutron diffraction remains limited. The X-ray photoelectron spectroscopy (XPS) valence spectrum of PITN has been found to be in good agreement with the theoretical curve calculated on the basis of an aromatic backbone.[11] However, the overall density of valence states, which is probed with XPS, is expected to be very similar for both quinoid and aromatic forms, so that such experimental data cannot provide the clear signature of one of the two structures. From Raman scattering data on neutral and doped PITN, it has been proposed that the ground-state geometric structure of the neutral system is quinoid and becomes aromatic upon doping.[12,13] This hypothesis is based on the comparison between the measured frequencies and values calculated for the quinoid and aromatic structures from the force constants of thiophene and benzene. However, the experimental Raman frequencies are in agreement with the calculated values for the aromatic structure of polythiophene only after a refinement procedure has been applied. When this procedure is used for PITN, the frequencies obtained for the aromatic and quinoid forms are so similar to each other that it seems very delicate to determine which set of results is closest to the experimental data. It thus appears that the question of the ground-state geometry of PITN is not resolved unequivocally by those results.

In this paper, we present a novel joint experimental and theoretical approach to investigate the structure of PITN and the relative stabilities of the two forms. We combine the results of NMR measurements performed on the polymer and on a series of selected molecular model compounds and the results of quantum-chemical calculations carried out on oligomers within the Austin model 1 (AM1) and valence effective Hamiltonian (VEH) methodologies.

2. General Approach

Due to the physical properties of PITN, the proper experimental technique to study its electronic structure must be applicable in the solid state and should be sensitive to small electronic changes such as those appearing between an aromatic and a quinoid form. With these constraints in mind, we started a solid-state ^{13}C NMR analysis of PITN.[14] High-resolution solid-state ^{13}C NMR spectra can be obtained with cross-polarization magic angle spinning (CP/MAS)[15] experiments, which combine high-power ^{1}H-decoupling, cross polarization (CP), and magic angle spinning (MAS). Sensitivity is enhanced by cross polarization[16] in which ^{1}H nuclear magnetization is transferred to ^{13}C in a double-resonance experiment under the Hartmann–Hahn[17] condition. Magic angle spinning[18] removes the chemical shift anisotropy and reduces proton–carbon dipolar interactions, thereby enhancing the resolution. But even under ideal experimental CP/MAS conditions, the resolution is limited by morphological disorder in amorphous materials. Another problem with regard to PITN concerns the small range in chemical shift of the inequivalent aromatic carbons. Therefore, a straightforward determination of the individual signals in a ^{13}C CP/MAS spectrum of the polymer is hindered by the overlap of the four contributions. To overcome this problem, we have used different selective solid-state NMR pulse sequences resulting in selective carbon polarization.

The first pulse sequence is the standard cross-polarization pulse sequence. During cross polarization, the large proton magnetization is used to polarize the ^{13}C nuclei. The CP rate (T_{CH}^{-1}) depends on r_{CH}^{-6}, so that the nonprotonated carbons cross polarize only slowly.[19] This disparity in CP rate can be turned to good use by running experiments as a function of the contact time (CT) to distinguish between protonated and nonprotonated carbons. A more rigorous distinction between protonated and nonprotonated carbons can be achieved with the proton-dephasing (PDP)[20] technique. In this case, selectivity is based on the difference in ^{13}C–H dipolar interaction due to the r_{CH}^{-3} dependence. Experimentally, a short delay (50 μs) with both the proton and the carbon channels off is inserted after cross polarization and before data acquisition. In order to further increase the selectivity, the cross-depolarization (CDP) technique[21,22] was used in combination with standard CP and PDP experiments. In the CDP pulse sequence, the ^{1}H radiofrequency phase is inverted for 0–5000 μs after the cross-polarization mixing period and prior to carbon observation. During this period, carbon spins cross polarize in the reversed direction. When the nonprotonated carbons are under investigation, an extra PDP delay is inserted between the CDP period and the carbon observation. The carbon magnetization varies in the following manner: it first decreases, vanishes at a certain moment, and then increases along the opposite direction. As the cross-depolarization time (td) is increased, the polarization of protonated lines is inverted first, due to their higher polarization-transfer rate. During the PDP time, the protonated carbons are suppressed by dephasing.

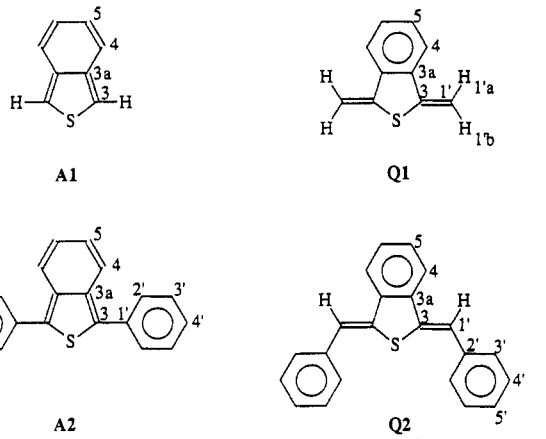

Figure 1. First-order [isothianaphthene (**A1**), 1,3-bis(methylene)benzo[*c*]thiophene (**Q1**)] and second-order [1,3-diphenylisothianaphthene (**A2**), 1,3-dibenzalthiophthalan (**Q2**)] model compounds.

To understand the chemical shift obtained on the polymer in terms of the structure of the PITN chain, we have synthesized a series of model isothianaphthene (ITN) molecules, unambiguously possessing either an aromatic or a quinoid geometric structure (Figure 1). Isothianaphthene (**A1**) and 1,3-bis(methylene)benzo[*c*]thiophene (**Q1**) can be considered as the basic structure units to model the aromatic or quinoid polymer chain, respectively; they will be referred to as the "first-order" model compounds. The addition of terminal phenyl rings to form 1,3-diphenylisothianaphthene (**A2**) and 1,3-dibenzalthiophthalan (**Q2**) allows for an improved description of the ITN unit inserted in a conjugated backbone; hereafter, they will be called "second-order" model compounds. The chemical shifts measured for these ITN derivatives are compared to the polymer data, and the structure of PITN is deduced on the basis of comparison.

In the theoretical part of this work, we calculate the geometric structure and the electronic properties of PITN and the parent polymer, polythiophene. The structure of the polymers is obtained from full geometry optimizations of oligomers of various chain lengths, performed with the

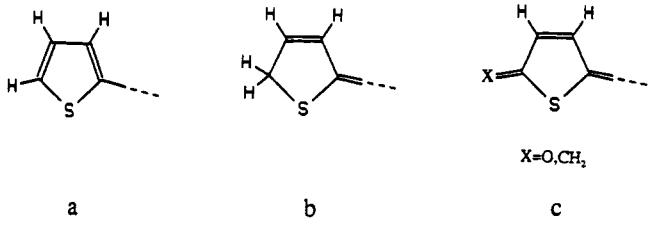

Figure 2. Illustration of the different chain ends considered for the polythiophene oligomers (the chain extends to the right-hand side of the structures).

AM1 method,[23] which was designed to provide accurate geometries and heats of formation, particularly for organic systems. With respect to MNDO, the AM1 technique provides a much improved description of the interaction taking place between nonbonded atoms, e.g., hydrogen-bonding or steric interactions. The latter are very important in aromatic conjugated systems since they determine the planarity or nonplanarity of the chain, hence its degree of π electron conjugation. The results of the AM1 calculations are also used to estimate the relative stabilities of the polymers in the two possible valence bond forms (aromatic and quinoid) of the conjugated backbone. The relative stability of the aromatic and quinoid forms of the polymers is estimated on the basis of the energy per repeat unit (E_{pru}). One approach to calculating E_{pru} is derived from the total energies (or heats of formation) in a series of oligomers.[24,25] It has been shown recently that, for conjugated systems, calculating $E_{pru}(N) = E(N) - E(N-1)$ provides good estimates of E_{pru}, even when short oligomers are considered;[9,26] this is due to the fast convergence of the total energy terms (N corresponding to the number of repeat units within the oligomer).

The AM1 geomerty optimizations are performed for ITN and thiophene oligomers using the MOPAC 6.0 package running on a IBM RISC/6000 workstation. We only consider systems where the rings are connected to each other through α- and α'-carbon positions, allowing for the strongest π electron conjugation to take place. In the case of thiophene, the optimizations are carried out on a series of N-mers of increasing length, from the monomer (N = 1), dimer (N = 2), trimer (N = 3), tetramer (N = 4), and hexamer (N = 6), to the decamer (N = 10). Due to the large size of ITN, the longest oligomer we consider in this series is the hexamer. In the first set of calculations, the ITN and thiophene oligomers are defect-free, with all carbon atoms being sp^2-hybridized (Figure 2a); the starting geometry is either aromatic or quinoid. We then stimulate chain-end defects by adding one hydrogen atom (Figure 2b) or by forming a terminal methylene (CH_2=) or carbonyl group (Figure 2c) on each of the terminal α-carbon sites. Again, we introduce either a quinoid or an aromatic structure as the starting geometry for the conjugated backbone. In all the calculations, the geometric structure is allowed to relax completely. To determine the effect of the torsion of the rings around the inter-ring bonds upon the electronic properties, we compare a totally planar conformation with one where the units are allowed to tilt with respect to each other.

The geometries and the relative stabilities obtained with AM1 are compared to the structure properties for PITN from the NMR investigations. Using the AM1-derived structural information as input, we also determine the most relevant electronic parameters of the polymer (bandgap, ionization potential, width of the highest occupied electronic band) from VEH band structure calculations. This technique is well-known to provide reliable estimates for the electronic properties of polymers,

Scheme I

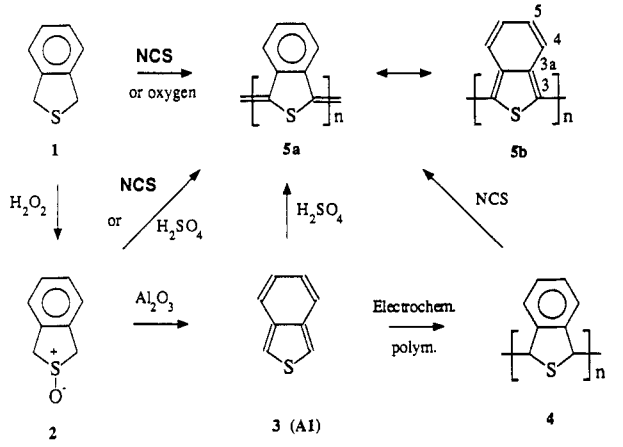

both conjugated and nonconjugated.[27-31] The geometry of the unit cell introduced in the VEH calculations corresponds to the AM1-optimized structure of the central part of the hexamer. As will be discussed below, AM1 is found to give too short values (ca. 1.42 Å) for the inter-ring bonds in aromatic systems, compared to the experimental values; the VEH calculations are therefore carried out with an inter-ring bond length set at 1.45 Å, a value corresponding to the results of X-ray diffraction measurements on thiophene oligomers.[32,33]

3. Experimental Section

A. Preparation of Polymer 5 (Scheme I). The monomer 1,3-dihydrobenzo[*c*]thiophene (1; 10 g, 73.4 mmol) was refluxed with *N*-chlorosuccinimide (NCS; 24.5 g, 183 mmol) in carbon tetrachloride for 1 h. After evaporation of the solvent, the residue was Soxhlet-extracted with ethyl alcohol, tetrahydrofuran, chloroform, and light petroleum, followed by drying under vacuum (90% yield based on the amoung of 1 used). The samples were dedoped in concentrated aqueous NH_3 for 20 h[34] (70% yield after reaction and dedoping): FT-IR (KBr, ν, cm^{-1}) 1678, 1587, 1452, 1377, 1259, 1219, 1188, 1138, 1049, 970, 874, 845, 737, 665. Anal. Calcd for $(C_8H_4S)\cdot(O)_{0.23}\cdot(Cl)_{0.04}\cdot(N)_{0.06}$: C, 71.43; H, 2.99; S, 23.83; O, 2.73; Cl, 1.05; N, 0.62. Found: C, 69.46; H, 2.93; S, 22.29; O, 2.72; Cl, 0.93; N, 0.58.

B. Preparation of the Model Compounds. (1) 1,3-Bis(methylene)benzo[*c*]thiophene (Q1). This first-order model compound for the quinoid structure **Q1** was synthesized according to the literature procedure.[35] Addition of sulfur dichloride to *o*-divinylbenzene yields a mixture of cis and trans isomers of 3,4-dihydro-1-(chloromethyl)-4-chloro-1*H*-2-benzothiopyran, which rearranges to 1,3-dihydro-1,3-bis(chloromethyl)benzo[*c*]thiophene (spontaneously or) by percolation through a silica gel column. Dehydrochlorination of the latter with 1,5-diazobicyclo[5.4.0]-undec-5-ene (DBU) yields the unstable 1,3-bis(methylene)-benzo[*c*]thiophene: ^{1}H-NMR (200 MHz, $CDCl_3$, δ relative to TMS) 7.62 (dd, 2, H4 and H7), 7.34 (dd, 2, H5 and H6), 5.74 (d, 1, H1'a), 5.22 (d, 1, H1'b); ^{13}C NMR (50.3 MHz, $CDCl_3$, δ relative to TMS) 144.3 (C3), 138.6 (C3a), 128.6 (C5), 120.9 (C4), 100.1 (C1').

(2) 1,3-Dibenzalthiophthalan 2-Oxide (6; Scheme II). Potassium (1.56 g) was added to 35 mL of *tert*-butyl alcohol (dried by refluxing with CaH_2) in a 250-mL three-neck flask under a stream of nitrogen (mercury trap). If the alcohol and apparatus are properly dried, the reaction of the potassium is slow, requiring 3–4 h at ~5 °C. After the addition of dry tetrahydrofuran (12 mL), the solution was cooled to 0 °C. A solution of 1,3-dihydrobenzo[*c*]thiophene 2-oxide (**2**; 1.52 g, 10 mmol) and benzaldehyde (6.37 g, 60 mmol) in 20 mL of *tert*-butyl alcohol and 12 mL of tetrahydrofuran was added dropwise over a period of 20 min. [Benzaldehyde was purified before use by washing with aqueous sodium hydroxide (10%), a saturated Na_2SO_3 solution, and water, dried over $CaCl_2$, and distilled under reduced pressure.] After being stirred overnight, the mixture was evaporated. Water was added to the residue, followed by

Scheme II

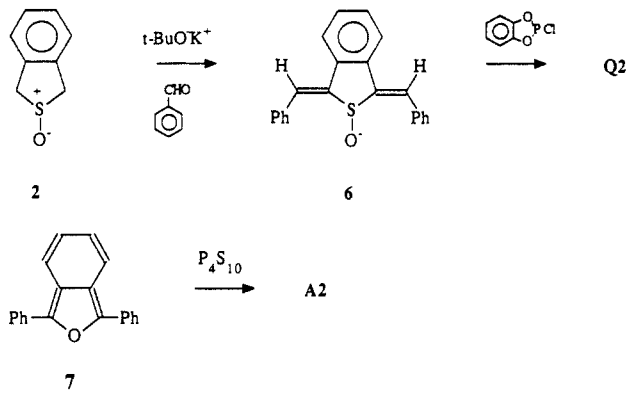

extraction with CH_2Cl_2. Finally, the organic layer was dried ($MgSO_4$) and evaporated. Column chromatography of the crude product on silica gel using chloroform/ethyl acetate (95:5) as eluant yielded 1,3-dibenzalthiophthalan 2-oxide (**6**; 90%) as an orange crystalline product: mp 196 °C dec; IR (KBr, ν, cm^{-1}) 3060 (w), 3000 (w), 1610 (w), 1570 (w), 1490 (m), 1450 (m), 1230 (m), 1180 (m), 1160 (m), 1080 (m), 1020 (s, ν_{S-O}), 930 (m), 890 (m), 860 (w), 840 (w), 760 (s), 700 (s), 600 (m), 550 (m), 500 (m), 460 (m), 430 (m), 350 (w); MS *m/e* (fragment rel intensity) 328 (25), 312 (85), 237 (100), 221 (30), 189 (15); ^{1}H NMR (400 MHz, $CDCl_3$, δ relative to TMS) 7.86 (d, 4, H3′ and H7′), 7.68 (dd, 2, H4 and H7), 7.61 (s, 2, H1′), 7.45 (t, 4, H4′ and H6′), 7.40 (dd, 2, H5 and H6), 7.38 (t, 2, H5′); ^{13}C NMR (100 MHz, $CDCl_3$, δ relative to TMS) 143.8 (C3), 136.1 (C3a), 134.6 (C2′), 132.8 (Cl′), 130.1 (C5), 130.0 (C3′), 129.6 (C5′), 129.0 (C4′), 122.1 (C4).

(3) 1,3-Dibenzalthiophthalan (Q2). To a stirring solution of 1,3-dibenzalthiophthalan 2-oxide; (**6**; 1.97 g, 6 mmol) and pyridine (0.47 g, 6 mmol) in dry benzene (6 mL) was slowly added 2-chloro-1,3,2-benzodioxaphosphole (1.05 g, 6 mmol). After 90 min, aqueous sodium hydroxide (2 N) was added and the benzene layer was washed several times with a sodium hydroxide solution, followed by one water wash. After drying (Na_2SO_4), the benzene was removed to yield the crude sulfide **Q2**. A very fast percolation through a silica gel column in chloroform yielded 1,3-dibenzalthiophthalan (**Q2**; 75%) as a yellow crystalline product. Bright yellow needles were obtained after recrystallization from ether/dichloromethane: mp 199–200 °C dec; IR (KBr, ν, cm^{-1}) 3060 (w), 3040 (w), 1600 (m), 1570 (w), 1490 (m), 1450 (m), 1300 (m), 1110 (m), 920 (m), 910 (m), 840 (m), 770 (s) 690 (s), 510 (m); MS *m/e* (fragment rel intensity) 312 (100), 278 (10), 234 (15), 221 (5); ^{1}H NMR (400 MHz, $CDCl_3$, δ relative to TMS) 7.83 (dd, 2, H4 and H7), 7.66 (d, 4, H3′ and H7′), 7.44 (t, 4, H4′ and H6′), 7.40 (dd, 2, H5 and H6), 7.26 (t, 2, H5′), 7.25 (s, 2, H1′); ^{13}C NMR (100 MHz, $CDCl_3$, δ relative to TMS) 139.1 (C3a), 136.8 (C3), 136.7 (C2′), 128.8 (C3′), 128.7 (C4′), 128.5 (C5), 127.0 (C5′), 120.8 (C4), 116.9 (C1′).

(4) 1,3-Diphenylisothianaphthene (A2). The synthesis of the aromatic model compound 1,3-diphenylisothianaphthene (**A2**) has been reported by Cava et al.[36] **A2** was recrystallized from ethyl alcohol to give yellow needle crystals: lit. mp 119–120 °C; IR (KBr, ν, cm^{-1}) 3060 (w), 1600 (m), 1480 (m), 1440 (m), 1200 (m), 1080 (w), 1040 (w), 910 (m), 770 (s), 700 (s), 580 (m); MS, *m/e* (fragment rel intensity) 286 (100), 252 (20), 165 (10), 143 (10), 126 (20); ^{1}H NMR (400 MHz, $CDCl_3$, δ relative to TMS) 7.88 (dd, 2, H4 and H7), 7.74 (d, 4, H2′ and H6′), 7.52 (t, 4, H3′ and H5′), 7.41 (t, 2, H4′), 7.13 (dd, 2, H5 and H6); ^{13}C NMR (400 MHz, $CDCl_3$, δ relative to TMS) 135.3 (C3a), 134.4 (C1′), 134.2 (C3), 129.3 (C2′), 129.0 (C3′), 127.4 (C4′), 124.2 (C5), 121.2 (C4).

C. Measurements. Solution ^{1}H and ^{13}C NMR spectra of the model compounds were obtained in $CDCl_3$ at 30 °C with a Varian Unity 400 spectrometer. As an internal standard, $CDCl_3$ and $CHCl_3$ (the chemical shifts of the carbon and the hydrogen being 77.0 and 7.24 ppm, respectively, from tetramethylsilane) were employed. The peaks in the ^{1}H NMR spectra were assigned from the results of selective irradiation and 2D-NOESY experiments. These ^{1}H chemical shift data were useful for the spectral assignment of the ^{13}C NMR spectra based on ^{13}C–^{1}H 2D correlation experiments optimized for J = 140 Hz and J = 8 Hz.

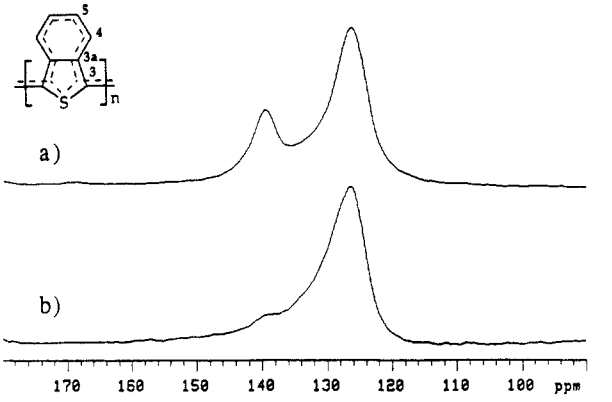

Figure 3. ^{13}C CP/MAS NMR spectra of PITN: (a) contact time CT = 1 ms; (b) CT = 50 μs.

All solid-state ^{13}C NMR spectra were recorded with a Varian XL-200 instrument (50.3 MHz). ^{13}C cross-polarization measurements used 25–5000-μs mixing times, high-power (44 kHz) ^{1}H decoupling, and recycle times of 2 s. Magic angle spinning was performed at 3.0–6.0 kHz using Si_3N_4 rotors. KBr was used to set the magic angle while the Hartmann–Hahn condition was adjusted using the aromatic signal to hexamethylbenzene. The chemical shift of this signal was employed as a standard (the shift of the aromatic signal being 132.1 ppm from TMS). Spectral assignment was facilitated with the aid of proton-dephasing, cross depolarization, and the combination of both techniques.

4. NMR Results

A. Synthesis of PITN 5. Several routes have already been developed for the chemical and electrochemical synthesis of PITN 5. Powders are obtained by chemical polymerization of several isothianaphthene precursors. The oxidative polymerization of isothianaphthene (**3**) and 1,3-dihydrobenzo[*c*]thiophene 2-oxide (**2**) using concentrated H_2SO_4 was reported by Wudl et al.[2] (Scheme I). Jen and Elsenbaumer discovered a procedure for the synthesis of **5** directly from 1,3-dihydrobenzo[*c*]thiophene (**1**) and oxygen or an other oxidant/dopant like ferric chloride.[37] This route eliminates the oxidation of **1** (and dehydration of the resulting sulfoxide **2**). The use of *N*-chlorosuccinimide has already been mentioned for the conversion of poly(dihydroisothianaphthene) **4** to PITN. The same reagent can be used for the conversion of the monomers **1** and **2** into PITN without first preparing **4**.[38] The reaction of the sulfide **1** with 1.2 equiv of NCS yields 48% PITN (based on the amount of **1** used). This conversion is restricted by the amount of NCS since a yield of 90% was obtained with 2.5 equiv of NCS. It should be noticed that the samples are obtained in the doped state in the latter case (based on the elemental analysis and the bandwidth in the ^{13}C CP/MAS NMR and FT-IR spectra).

B. NMR Analysis of PITN 5. All the ^{13}C CP/MAS NMR spectra of PITN presented here were taken of the polymer **5** obtained from the sulfide **1** with 2.5 equiv of NCS (after dedoping). Figure 3 shows ^{13}C CP/MAS NMR spectra of **5** with a contact time of 1 ms (a) and 50 μs (b). The peak at 139 ppm in spectrum a can be assigned to a nonprotonated carbon since it is not present in the spectrum with CT = 50 μs. In the latter spectrum, one asymmetric signal can be observed with a maximum at 126.5 ppm. This signal is attributed to one or more protonated carbons because of the very short contact time.

In the PDP spectrum of **5** previously reported,[14] a contact time of 1 ms was used. Besides the signal at 139 ppm and the shoulder at ±134 ppm (both attributed to the nonprotonated carbons of **5**), a peak at 125–126 ppm can

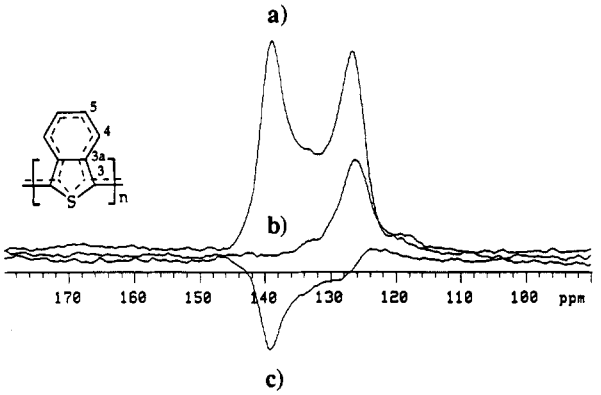

Figure 4. Proton cross-dephasing depolarization ^{13}C CP/MAS NMR spectra of PITN with CT = 5 ms and increasing depolarization time, td = 0 (a), 800 (b), and 2000 (c) μs.

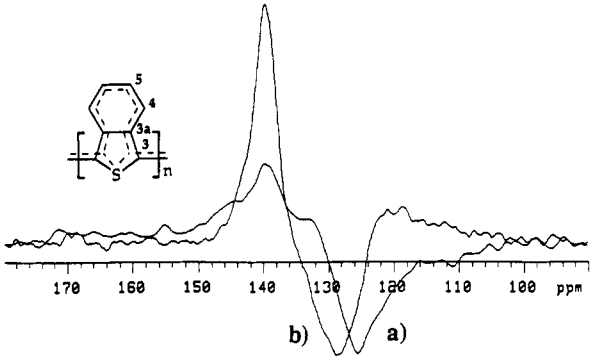

Figure 5. Cross-depolarization ^{13}C CP/MAS NMR spectra of PITN with CT = 50 μs and td = 44 μs (a) and with CT = 300 μs and td = 50 μs (b).

be seen from this spectrum. Initially, we considered the latter resonance to be a nontotally suppressed protonated signal since the position corresponds to the resonance in the spectrum generated with a very short contact time (50 μs). Figure 4 shows a PDP spectrum of **5** using a rather long contact time of 5 ms (a). Two signals at 139 and 126 ppm can be seen in this spectrum, the latter being much more intense than in the previously reported spectrum with CT = 1 ms. An explanation for this observation is that the signal at 126 ppm arises from a nonprotonated carbon which cross polarizes very slowly due to the large average C–H distance. Consequently, a contact time of 5 ms may be the proper contact time for this signal. In order to test this hypothesis, we performed an experiment in which cross depolarization and proton dephasing are combined. After depolarization for a time td, the resulting magnetization of the protonated carbons is dephased during the PDP sequence. From the other spectra in Figure 4, it can be seen that the signal at 139 ppm disappears (td = 800 μs) while the resonance at 126 ppm is still positive (b). For the latter to become zero, a depolarization time of 2 ms is necessary (c). The fact that the signal at 126 ppm cross polarizes even more slowly than the signal at 139 ppm proves that we are dealing with a nonprotonated carbon. This experiment is necessary since the position of one nonprotonated carbon corresponds to the shift of one or more protonated carbons (cf CP/MAS spectrum with CT = 50 μs). The significantly slower cross depolarization of the signal at 126 ppm compared to the resonance at 139 ppm suggests a larger distance to the surrounding hydrogens, which points to C3 at 126 ppm. As a consequence, the chemical shifts of the nonprotonated carbons C3 and C3a of **5** are 126 and 139 ppm (±0.5 ppm), respectively. It is also important to stress that the nonprotonated line at 134 ppm (±2 ppm – shoulder), previously assigned to C3 or C3a, probably arises from structural defects which are not well-characterized at this moment.

In order to separate the lines of the protonated carbons C4 and C5 of PITN, we first perform cross-depolarization experiments with a contact time of 1 ms.[38] When a depolarization time of 175 μs is used, a signal at 125 ppm can be observed. With such a contact time (cf. PDP with CT = 1 ms[14]), however we cannot exclude the contribution of the nonprotonated line at 126 ppm (considering the results of the CDP–PDP combination). We therefore select experimental conditions in which the contribution of the quaternary carbon at 126 ppm can be excluded. This can be realized with cross-depolarization spectra using only a very short contact time (50 μs). In the ^{13}C CP/MAS spectrum with this contact time (Figure 3b), the resonance at 139 ppm is negligible. Certainly, this is by all means the case for the other quaternary carbon (at 126 ppm), due to its slower cross polarization. A CDP/MAS spectrum of **5** with a CT = 50 μs and a depolarization time of 44 μs is presented in Figure 5a. In our opinion, there is a small contribution of other protonated carbons to this resonance resulting in a small variation of the maximum when depolarization time varies. As a consequence, the chemical shift of the protonated lines cannot be determined with the same accuracy as for the quaternary carbons. From the signal in Figure 5a, an average chemical shift of 125 ± 1 ppm is determined. The other protonated line can be seen from a CDP/MAS spectrum with a contact time of 300 μs and a depolarization time of 50 μs (Figure 5b). A chemical shift of 128.5 ± 1 ppm is estimated for this signal.

Even when the ^{13}C chemical shifts of the inequivalent carbons of PITN are known, no conclusion about its geometric structure can be drawn. To achieve this goal, chemical shift data of model compounds for aromatic and quinoid structures are necessary.

C. First- and Second-Order Model Compounds: A1, Q1, A2, and Q2. The chemical shifts measured on the first-order model compound with a quinoid structure, 1,3-bis(methylene)benzo[*c*]thiophene (**Q1**)[39] are summarized in the Experimental Section. The data for the first-order aromatic model compound isothianaphthene (**A1**) are taken from the literature.[40]

The synthesis of the second-order quinoid model compound 1,3-dibenzalthiophthalan (**Q2**) starting from thiophthalic anhydride and benzylmagnesium chloride has been described by Omran and Harb.[41] Unfortunately, no ^{13}C chemical shifts are available from that report, and the yield and the purity of **Q2** were not satisfactory in our experiments. We therefore developed a new synthetic route for this model compound (see Scheme II): 1,3-dibenzalthiophthalan 2-oxide (**6**) is reduced with 2-chloro-1,3,2-benzodioxaphosphole[42] to the corresponding sulfide **Q2**. The sequence oxidation–condensation–reduction is necessary to enhance the acidity of the hydrogens on the 1 (and 3) position. We have observed that the condensation cannot be carried out with 1,3-dihydrobenzo[*c*]-thiophene (**1**).

We now focus on the ^{1}H NMR spectrum of **Q2** (entry F1 on Figure 6) since these data are necessary for the ^{13}C NMR analysis. We assign this spectrum on the basis of the coupling patterns. The only absorption without a vicinal ($^{3}J_{HH}$) coupling (7.25 ppm) corresponds to H1′. The doublet at 7.66 ppm can be assigned to H3′. The integration was used to distinguish between the two triplets at 7.44 and 7.26 ppm arising from H4′ and H5′, respectively. The remaining two patterns (dd) at 7.83 and 7.40 ppm are attributed to protons H4 and H5. A distinction could be

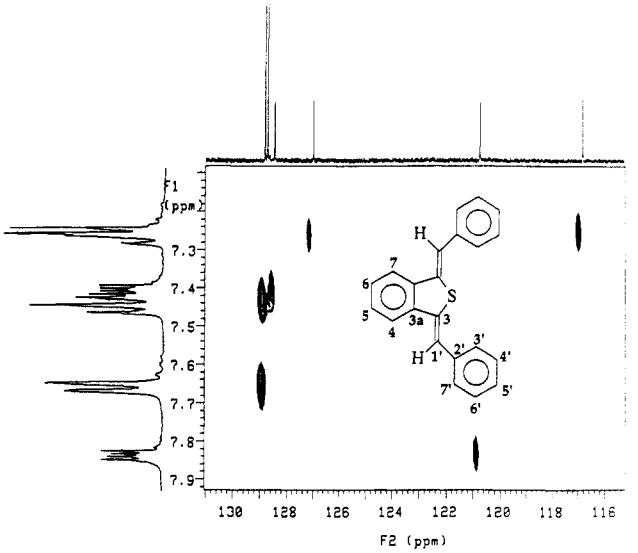

Figure 6. 2D heteronuclear $^{13}C-^{1}H$ correlation spectrum of **Q2** optimized for J_{CH} = 140 Hz ($CDCl_3$ 30 °C).

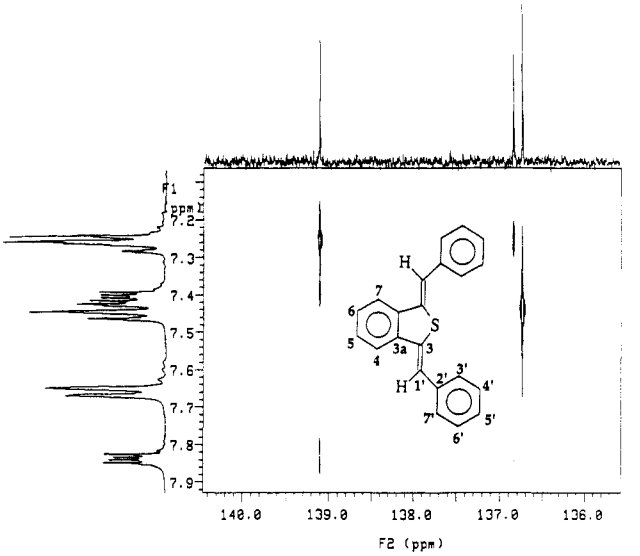

Figure 7. 2D heteronuclear $^{13}C-^{1}H$ correlation spectrum of **Q2** optimized for J_{CH} = 8 Hz ($CDCl_3$ 30 °C).

made based on a NOE effect (due to the proximity) between H4 and H1′. We assigned the pattern at 7.83 ppm to H4 with a double-resonance experiment in which H1′ was selectively irradiated. This conclusion was confirmed by a 2D-NOESY experiment. These NOE experiments make clear that the condensation reaction of the sulfoxide **2** with benzaldehyde leads to the sterically less hindered product (both phenyl rings being trans with respect to the benzo[*c*]thiophene six-membered ring).

For the assignment of the ^{13}C NMR spectrum of **Q2**, the peaks were classified into two groups (i.e., the peaks due to the protonated carbons and the peaks due to the nonprotonated carbons) with the aid of a ^{13}C spectrum without decoupling. The heteronuclear coupling patterns in this spectrum are insufficient for the full assignment of the ^{13}C spectrum because of overlap and second-order effects. An unambiguous assignment is, however, necessary since the chemical shifts of carbons C3, C3a, C4, and C5 are to be compared to PITN. The protonated lines were assigned from the results of a heteronuclear $^{13}C-^{1}H$ 2D correlation experiment optimized for ^{1}J = 140 Hz (Figure 6). From this spectrum it can be seen that the pattern at 7.83 ppm (=δH4 > δH5) corresponds to the ^{13}C resonance at 120.8 ppm (=δC4 < δC5). To distinguish between the nonprotonated carbons C2′, C3, and C3a, we employed a similar heteronuclear correlation experiment optimized for a geminal ($^{2}J_{CH}$) or a vicinal ($^{3}J_{CH}$) coupling (J = 8 Hz). This spectrum is shown in Figure 7. A correlation can be observed for the carbon resonance at 139.1 ppm and H1′ (s, 7.25 ppm), H4 (dd, 7.83 ppm), and H5 (dd, 7.40 ppm). The carbon C3a is the only atom that meets this condition. C2′ being the only carbon which can correlate with H4′ (t, 7.44 ppm), it corresponds to the resonance at 136.7 ppm. The remaining signal (136.8 ppm) is attributed to C3, which is confirmed by its correlation with H1′ (s, 7.25 ppm) and H4 (dd, 7.83 ppm).

The ^{13}C chemical shifts of the second-order aromatic model compound **A2** reported by Cohen et al.[43] and Volz and Voss[44] are inconsistent. We therefore reinvestigated the NMR analysis of **A2**, employing the same procedure as described above. The assignment of the ^{1}H spectrum was based on the coupling patterns. A 1D double-resonance NOE experiment was necessary to distinguish between H4 and H5 (based on the proximity of the protons H4 and H2′). The peaks in the ^{13}C spectrum were assigned with the aid of $^{13}C-^{1}H$ correlation experiments.

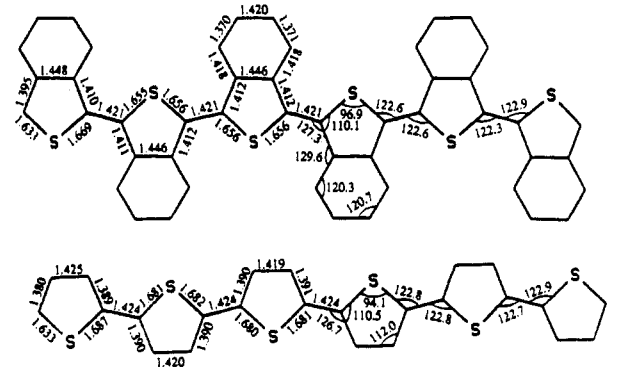

Figure 8. AM1-optimized geometry for the planar aromatic structures of ITN and thiophene hexamers (bond lengths in angstroms; bond angles in degrees).

The chemical shifts of C3, C3a, C4, and C5 ($CDCl_3$) in the second-order aromatic and quinoid model compounds can be compared to the values of PITN. Since PITN is insoluble, only data determined in the solid state are available. Therefore, we tried to determine ^{13}C chemical shifts of the model compounds in the solid state. For compound **Q2**, it was not possible to determine the ^{13}C shift of C5 due to overlap with the signals of the phenyl side group. The ^{13}C shifts in the solid state for C4, C3, and C3a (120.0, 136.0, and 140.0 ppm, respectively) correspond well with the values determined in $CDCl_3$ (120.8, 136.8, and 139.1 ppm). For the aromatic model compound **A2**, a maximum difference of 2 ppm between the shift in the solid state and the liquid phase is observed for C3. For the other carbons, the difference remains within 1 ppm (see below).

5. Theoretical Results

A. Geometric Structure. In the case of defect-free systems (Figure 2a), the optimized geometric structure is calculated to be aromatic, for both thiophene and ITN oligomers, independent from the nature of the starting geometry. The structures of the two hexamers in the planar conformation are shown in Figure 8. The C–S bonds are 0.020–0.025 Å shorter in ITN oligomers than in their thiophene counterparts, which can in principle be related to the existence of a resonance form of ITN having C–S double bonds.[5]

The carbon–carbon bond-length alternation within the five-membered rings is found to be rather small, 0.03 Å,

which is about half the value obtained on thiophene and ITN oligomers with MNDO[5] and PRDDO.[8] The AM1-calculated inter-ring bond length (1.42 Å) also appears slightly shorter compared to previous predictions. This reduced bond-length alternation is not an effect of the benzene ring fusion upon the thiophene unit, as it is observed for both thiophene and ITN compounds. Instead, it must be considered as a feature typical of the AM1 parameterization. Besides this shortcoming, the most important point is that the bond-length alternation, albeit small, remains constant as the oligomers get longer. On the one hand, the bond-length alternation of long oligomers ($N = 6$ for ITN, $N = 10$ for thiophene) is identical to that of the dimers and the trimers. On the other hand, no significant evolution is observed along the backbone of long ITN oligomers, as seen in Figure 8. This is in marked contrast to the results of Hückel-type calculations.[10] From the Hückel results, it was proposed that the geometric structure of defect-free ITN oligomers is quinoid for $N > 8$, a trend already observed in the central segment of shorter oligomers. This behavior is *not* confirmed by the Hartree–Fock AM1 calculations we are using in this work. It should be noted that more sophisticated ab initio methods also predict that the geometric structure of long defect-free ITN oligomers up to the pentamer remains completely aromatic.[45] Probably the parameterization of the Hückel Hamiltonian used in ref 10 overestimates the stabilization of the quinoid form relative to the aromatic form.

As already pointed out previously,[6,8] steric interaction between the sulfur atom and one hydrogen atom from the neighboring benzene rings is likely to prevent an aromatic PITN chain from being fully planar. The dihedral angle between the planes of adjacent ITN units is found to be 27° at the AM1 level; this is much smaller than the value determined with MNDO (85°),[6] which is a consequence of the poorer capabilities of the MNDO method in the description of nonbonded interactions. The PRDDO approach yields a somewhat intermediate value of 59°.[8] The bond lengths and bond angles of the twisted systems are in all cases very close to the corresponding values in the planar oligomers: the maximum difference in bond lengths is 0.002 Å and the bond angles do not differ by more than 0.5°. However, the existence of a nonzero dihedral angle may be more relevant for the energetic aspects and the electronic properties of ITN oligomers in the aromatic form (see below).

Compared to the defect-free systems, the geometric structure of the sp^3-terminated ITN and thiophene oligomers (Figure 2b) shows a reversed bond-length alternation and becomes quinoid: the α–β bond lengths increase by 0.06 and 0.04 Å in thiophene and ITN systems, respectively, whereas the inter-ring bonds shorten from 1.42 to 1.35 Å (Figure 9). As a consequence of the double-bond character of the inter-ring bond, the oligomers are totally coplanar in all cases, even though the S–H contact is as short as 2.24 Å. The quinoid form can also be induced by substituting the hydrogen atom on the terminal α-carbon with a methylene (CH_2=) group (Figure 2c, X = CH_2), as proposed in the literature,[8,9] or by forming a carbonyl group on the terminal carbon (Figure 2c, X = O). We find that the AM1-calculated geometries for the CH_2= substituted and C=O-terminated systems are identical to those of the sp^3-terminated oligomers (the only difference being that the terminal α–β carbon–carbon bonds are slightly shorter in the former systems).

The evolution of the bond lengths within the ITN unit can be related to the change in the bonding–antibonding pattern of the highest occupied molecular orbital (HOMO)[4a,46,47] when going from the aromatic to the quinoid geometric structure, as this pattern usually reflects the ground-state geometry in conjugated compounds. The change in the HOMO electronic structure can also be used to rationalize the increase of the C–S bond length in the quinoid forms relative to the aromatic forms, since a nonbonding situation in the aromatic pattern is replaced by an antibonding interaction between the two sites in the quinoid HOMO. The C–C bond-length alternation within the ring determined with AM1 on the ITN systems appears to be closer to the MNDO results[6] than to the PRDDO approach.[8] The latter predicts a 0.11-Å difference in bond length between the α–β and β–β' carbon–carbon bonds, while in AM1 and MNDO, the corresponding values are only 0.04 and 0.03 Å, respectively. Nevertheless, the three methods provide the same description of the basic structural features of quinoid ITN oligomers, in particular a very short inter-ring bond (1.35 ± 0.01 Å).

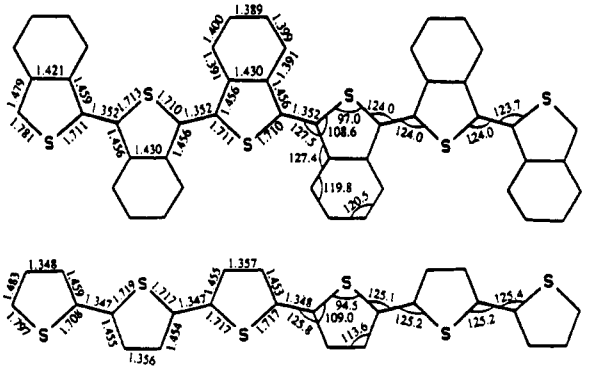

Figure 9. AM1-optimized geometry for the quinoid structures of ITN and thiophene hexamers (bond lengths in angstroms; bond angles in degrees).

Table I
Energy per Repeat Unit, $E_{pru}(N)$, for ITN and Thiophene Oligomers in the Aromatic (A) and Quinoid (Q) Forms

	$E_{pru}(N)$, kcal/mol			
	$N = 2$	$N = 3$	$N = 4$	$N = 6$
ITN (A)				
planar	51.8	52.0	51.8	51.4
27° tilted	51.2	51.4	51.2	51.3
ITN (Q)	48.8	49.1	49.0	49.1
thiophene (A)	29.1	29.1	29.1	29.2
thiophene (Q)	37.6	37.9	37.8	37.9

B. Energetic Aspects. The relative stability of the two forms of PITN and polythiophene can be estimated from the values of the energy per repeat unit (E_{pru}) of the oligomers collected in Table I. In all cases, the E_{pru} (N) values appear to converge quickly as the chain gets longer, as was also observed at the MNDO level.[9] For PITN, the energies of the quinoid and the aromatic geometric structures are very close, with the former slightly more favorable. The planar aromatic form is on the average 2.7 kcal/mol less stable than the quinoid form. This value is very close to the extrapolation of PRDDO results to the infinite chain limit: ΔE = 2.4 kcal/mol in favor of the quinoid form.[8] Allowing the ITN units to rotate around the inter-ring single bonds (to an average optimal dihedral angle of 27°) induces a small stabilization of the aromatic ITN oligomers, of the order of 0.5 kcal/mol per repeat unit. This stabilization reduces the energy difference between the two valence bond isomeric forms to 2.2 kcal/mol. The MNDO data[9] indicate that quinoid ITN oligomers are favored over their planar aromatic counterparts (ΔE = 7 kcal/mol) but the nonplanar aromatic structures are almost isoenergetic to the quinoid form ($\Delta E \approx 0.5$ kcal/mol).

Table II
VEH-Calculated Bandgap Energy (E_g), Ionization Potential (IP), and Width of the Highest Occupied Electronic Band (BW) for PITN and Polythiophene (PTh) in the Aromatic (A) and Quinoid (Q) Forms[a]

	E_g	IP	BW
PITN (A)[b]			
planar	0.21	3.83	2.89
27° tilted	0.61	4.31	2.33
PITN (Q)	1.19	4.35	2.39
PTh (A)[b]			
planar	1.59	4.68	2.54
27° tilted	1.68	4.97	2.12
PTh (Q)	0.26	3.98	3.47

[a] All values are in electronvolts. [b] Inter-ring bond length, 1.45 Å.

Table III
^{13}C Chemical Shifts (C3, C3a, C4, and C5) of PITN, the First- and Second-Order Model Compounds for an Aromatic and a Quinoid Structure (A1, Q1, A2, and Q2).

	δ, ppm			
	C3	C3a	C4	C5
A1[a]	116.4	138.0	121.8	123.4
A2[a]	134.2	135.3	121.2	124.2
A2[b]	132.5[c]	134.5	121.0	125.0[c]
PITN[b]	**126** ● 0.5	**139** ● 0.5	**125** ● 1	**128.5** ± 1
Q2[a]	136.8	139.1	120.8	128.5
Q2[b]	136.0	140.0	120.0[c]	
Q1[a]	144.3	138.6	120.9	128.6

[a] Measured in $CDCl_3$ (30 °C). [b] Measured in the solid state. [c] Shoulder.

As expected, the situation is much more clear-cut for polythiophene: the aromatic geometric structure is unequivocally more stable than the quinoid one. The energy difference between the two forms is calculated to be 8.7 kcal/mol per repeat unit at the AM1 level, very close to the value found with ab initio Hartree–Fock split-valence technique (8.0 kcal/mol.[9]). Similarly, the extrapolation of the energy difference to an infinite chain based on PRDDO calculations leads to a value of 10.4 kcal/mol[8] while the ΔE_{pru} obtained with MNDO is significantly smaller, 4.5 kcal/mol.[9]

It is to be noted that the optimized geometry of long sp^3-terminated thiophene oligomers, up to $N = 10$, remains totally quinoid, even though it is clearly established that the most stable situation for polythiophene is the aromatic form. This is observed even when starting from an aromatic geometry. The persistence of the quinoid structure probably arises from the fact that the formation of an aromatic segment in the central part of the sp^3-terminated system would induce the appearance of two unpaired electrons. Indeed, we observe that allowing the system to evolve toward a biradical structure, by going beyond the restricted Hartree–Fock formalism, leads to a more stable final structure for the longest oligomer. The bond-length alternation in the central segments of the molecule is reversed from quinoid to aromatic, and the radicals are located on each terminal thiophene unit. In the case of the sp^3-terminated hexamer, the biradical structure is favored by ≈15 kcal/mol over the fully quinoid one, due to the bond length reversal in the four central units.

C. Electronic Structure. In Table II, we compare the bandgap (E_g), ionization potential (IP), and valence bandwidth (BW) of PITN and polythiophene calculated with VEH on the basis of the AM1 geometry of the hexamers. In the planar aromatic form, PITN shows a very small bandgap (0.21 eV) while the value found for the quinoid polymer is much larger (1.19 eV). In the nonplanar aromatic form (with an average dihedral angle of 27°), the bandgap increases to 0.6 eV due to the partial loss of π conjugation. That value would correspond to that of a single PITN chain "in the gas phase". Most probably, the solid-state packing would somewhat reduce the tilt angle between adjacent ITN units, thereby leading to a slightly smaller value of the bandgap. On the basis of these results, aromatic and quinoid PITN are therefore predicted to present markedly different optical signatures, and the value for quinoid PITN is in better agreement with the bandgap derived from optical spectroscopy (onset of the spectrum located at 1.0 eV; maximum absorption at 1.5–1.6 eV).[48] This agreement further suggests that PITN possesses a quinoid structure. The bandgap we obtain for the quinoid form is also very close to the value calculated by Lee and Kertesz (1.16 eV[6]); the PRDDO/extended Hückel approach of Nayak and Marynick gives a smaller bandgap (0.8 eV[8]), as is usually the case with EHT.[49] The VEH bandgap of aromatic polythiophene with 1.45-Å inter-ring bonds is around 1.6–1.7 eV, close to the experimental value (2.0 eV[50]), while a polythiophene system with a quinoid backbone would possess a 0.26-eV bandgap. This result further confirms the aromatic character of polythiophene.

The ionization potentials listed in Table II are the energies of the top of the valence band corrected by substracting 2.3 eV to the calculated value to account for solid-state polarization effects; this allows for a better comparison with electrochemical data and with the binding energies measured with photoelectron spectroscopy. Here, only the IP value of PITN relative to other polymers will be discussed. The value calculated for quinoid PITN is ≈0.3 eV smaller than that of aromatic polythiophene. This is consistent with cyclic voltammetry curves which show a peak at 0.6 V vs the saturated calomel electrode for PITN[48] while the corresponding peak is located near 1.0 V in the case of polythiophene.[51]

Finally, the highest occupied bandwidth, which offers a qualitative insight into the mobility of the carriers along the conjugated backbone, is larger for the lowest bandgap, but least stable, forms: aromatic PITN (2.3–2.9 eV) and quinoid polythiophene (3.5 eV). However, the values found for the other two systems are still sufficient to allow for high carrier mobility. Furthermore, the bandwidth value for quinoid PITN (2.4 eV) is very close to that of aromatic polythiophene (2.1–2.5 eV), indicating that in principle PITN might show the same level of conductivity as its parent polymer.

6. Discussion

The ^{13}C chemical shift (C3, C3a, C4, and C5; in $CDCl_3$) of the first-order model compounds and PITN, measured in the solid state, are shown in Table III. The shift of C3a has approximately the same value in both compounds and in PITN whereas a significant difference between the models and the polymer can be seen for δC3 and δC4. The shift of C5 in **Q1** corresponds to the value of **5** while a difference of ≈5 ppm is observed for the same carbon in **A1**. From these data, no conclusion can be drawn in relation to the geometric structure of **5**, due to the fact that these model compounds do not represent the structure of PITN well enough. In the polymer, the chemical shift of the carbons of the benzo[c]thiophene skeleton is also determined by the neighboring aromatic rings. The situation is significantly different in the first-order model compounds, where the benzo[c]thiophene skeletons are not part of a conjugated π system (no neighboring rings).

Therefore, this simulation had to be improved by choosing new model compounds.

In the second-order compounds **A2** and **Q2**, the benzo[*c*]thiophene skeleton bears phenyl side groups. These aromatic rings simulate the neighboring unit in polymer **5**. The chemical shifts of the carbons of the benzo[*c*]thiophene skeleton of these second-order model compounds and PITN are also listed in Table III. Although the first-order model compounds (**A1** and **Q1**) were insufficient for the comparison to PITN, they can be used to determine the influence of the introduction of an aromatic phenyl group on the chemical shift of the carbons of the benzo[*c*]thiophene skeleton.

When we compare the ^{13}C shift of a certain carbon in **A2** and **Q2**, a significant difference can be observed for C3a and C5. The shift of these atoms seems to be a selective criteron for the geometric structure, and they are therefore very useful for the comparison with PITN. When the chemical shifts of C3a and C5 in **A2** and in **5** are compared, a significant difference of about 3–4 ppm can be observed (assuming that $\delta C5 > \delta C4$ and $\delta C3a > \delta C3$ for PITN, based on the same feature in all model compounds). However, the shift of these carbons corresponds very well to the values for quinoid model compound **Q2**. If the first- and second-order model compounds are compared, we notice that $\delta C3$ and $\delta C5$ are only slightly affected by the introduction of an aromatic side group (except for $\delta C3$ in **A2**), emphasizing the usefulness of these shifts as a criterion for the geometric structure.

When we focus on C3, the chemical shift of this carbon is strongly affected by the introduction of an aromatic side group in both the aromatic and quinoid structures, as expected when substitution is carried out in the 3-position. But even for the second-order model compounds **A2** and **Q2**, there is a difference of 7–10 ppm for $\delta C3$ in PITN and in both models. This can be explained by the fact that $\delta C3$ in **5** is also influenced by the sulfur atom of the neighboring ring (electronic interaction through the bonds). This situation is not accounted for by the second-order model compounds since there are no sulfur atoms in the aromatic side groups.

Finally, the shift of C4 in both **A2** and **Q2** differs from the value of PITN. Knowing that the chemical shift is also sensitive to electronic interactions through space, we can expect an influence of the sulfur atoms on the shift of C4 in the neighboring ring (due to the proximity of S and H4). Since the second-order model compounds do not bear sulfur atoms in the side groups, $\delta C4$ is not suitable for the comparison with PITN. The major difference in electronic interaction (through space) with H4 between PITN (quinoid structure) and **Q2** is caused by the difference in van der Waals radius between sulfur, which is present in the polymer, and hydrogen (H1′ and **Q2**).

From the comparison of the ^{13}C chemical shifts of PITN with those of model compounds for an aromatic and a quinoid structure, it therefore appears that: (i) there is no correspondence whatsoever between PITN and the aromatic model compounds; (ii) the shifts of C3a and C5 in **Q2** are in nice agreement with the polymer data; and (iii) this is not the case for C3 and C4, as the chemical environment of these sites is markedly different in **Q2** compared to the polymer. On the basis of these results, we propose that the geometric structure of PITN possesses a strong quinoid character.

The NMR data thus point toward a high quinoid contribution to the geometric structure of PITN, and the quantum-chemical calculations indicate that this structure is more stable than its aromatic counterpart. The bandgap calculated for quinoid PITN is in better agreement with the optical spectrum than the value calculated for the aromatic form. In our opinion, this combination of experimental and theoretical results represents strong evidence in favor of the existence of a quinoid geometric structure for PITN and confirms previous theoretical calculations.[6,8,9]

Another major feature appearing from the calculations is the small energy difference between the quinoid and the aromatic forms (≈2 kcal/mol per repeat unit). Since this is also observed with other theoretical methods, this small difference is to be considered an intrinsic characteristic of the PITN system. With such a small stability difference, it would be unwise to dismiss completely the possibility of also obtaining an aromatic PITN structure. The general question arising at this point is to establish to what extent the geometry of the polymer chain is determined by the energy difference between the aromatic and the quinoid geometric structures. The quantum calculations have shown that the nature of the end groups and the structure of the chain are directly related. Defect-free systems correspond to the aromatic geometric structure while the presence of sp^3 defects (Figure 2b) or sp^2 end groups (Figure 2c) is related to the quinoid form. In the case of the polythiophene, as the energy difference between the two forms is large (8.7 kcal/mol per repeat unit), quinoid oligomers of increasing length rapidly become less and less stable relative to their aromatic counterparts. For a certain chain length, one thus expects that an alternative structure possessing an aromatic character and two unpaired electrons be favored over the quinoid form, as shown above. Therefore, long quinoid oligothiophenes are not expected to exist, a situation that can be considered as typical of systems where the energy difference between the two forms is large.

In contrast, the quinoid and aromatic forms of PITN are almost isoenergetic; consequently, both structures are predicted to be much more stable than the hypothetical diradical intermediate. Therefore, depending on the chemical strategy chosen for the polymerization, one can select the structure which will be obtained, with small probability of crossing over to the other form through the high-energy diradical species. In this situation, the polymerization mechanism and the nature of the monomer and of the end groups can orient the synthesis. In this work, the starting compound is the partially saturated dihydro derivative and the polymerization is carried out oxidatively. Under these conditions, it is likely that chain ends consist of unreacted sp^3-hybridized sites, or that oxygen-containing groups, such as C=O, are formed on the terminal carbons. According to the calculations, the presence of these end groups is strongly related to the existence of the quinoid geometric structure. Therefore, the structure of the PITN polymer studied in this work is most probably quinoid, on the basis of the NMR data, the calculated total energies, and the chemical route used for the polymerization.

On the same basis, altering the synthetic conditions can lead to PITN with an aromatic geometric structure, as demonstrated very recently by Okuda et al.[52] who prepared the aromatic tetramer using a trimethylsilyl-substituted monomer. Aromatic PITN is certainly worthwhile to investigate, as the VEH results confirm that it should possess even smaller a bandgap than the quinoid form.

7. Synopsis

Solid-state ^{13}C NMR appears to be a powerful tool for determining the ground-state geometric structure of

conjugated polymers, in this particular case, PITN. From the analysis of the polymer and of a series of ITN derivatives, we have shown that the chemical shift of C5 and C3a in the second-order model compounds (with phenyl side groups) constitutes a selective criterion, indicating that the structure of PITN possesses a high quinoid character. We are currently exploring the synthesis of new model compounds, in which the chemical environment of C3 and C4 is comparable to the situation in the polymer, in order to confirm from NMR the results of this study. Nevertheless, the present results are already strongly supported by the quantum-chemical calculations, which indicate that the quinoid form is the most stable and that its calculated electronic properties are in good agreement with the experimental data. Finally, the theoretical calculations suggest that aromatic PITN could exist and that its bandgap may be even smaller than the value observed so far in the polymer with a quinoid geometry.

Acknowledgment. This work is partly supported by the Belgian Pôles d'Attraction Interuniversitaires Program 16. Research on polymers at Université de Mons-Hainaut is supported by Service de Programmation de la Politique Scientifique (SPPS, Contract IT/SC/22) and Fonds National de la Recherche Scientifique. I.H. is indebted to the Instituut tot aanmoediging van Wetenschappelijk Onderzoek in Nijverheid en Landbouw (IWONL) for a predoctoral fellowship.

References and Notes

(1) For recent reviews, see: Proceedings of the International Conference on Science and Technology of Synthetic Metals, Tübingen, September 2–7 1990; *Synth. Met.* **1991**, 41–43. *Conjugated Polymers*; Brédas, J. L., Silbey, R., Eds.; Kluwer: Dordrecht, The Netherlands, 1991.
(2) Wudl, F.; Kobayashi, M.; Heeger, A. J. *J. Org. Chem.* **1984**, *49*, 3382.
(3) Brédas, J. L. *J. Chem. Phys.* **1985**, *82*, 3808.
(4) (a) Brédas, J. L.; Heeger, A. J.; Wudl, F. *J. Chem. Phys.* **1986**, *85*, 4673. (b) Becker, R.; Blöchl, G.; Bräunling, H. In *Conjugated Polymeric Materials: Opportunities in Electronics, Optoelectronics, and Molecular Electronics*; Brédas, J. L., Chance, R. R., Eds.; NATO ASI Series E182; Kluwer: Dordrecht, The Netherlands, 1990; p 133. (c) Bräunling, H.; Becker, R.; Blöchl, G. *Synth. Met.* **1981**, *41*, 487. (d) Toussaint, J. M.; Wudl, F.; Brédas, J. L. *J. Chem. Phys.* **1989**, *91*, 1783. (e) Toussaint, J. M.; Brédas, J. L. *J. Chem. Phys.* **1991**, *94*, 8122.
(5) Brédas, J. L.; Thémans, B.; André, J. M.; Heeger, A. J.; Wudl, F. *Synth. Met.* **1985**, *11*, 343.
(6) Lee, Y.; Kertesz, M. *J. Chem. Phys.* **1988**, *88*, 2609.
(7) Brédas, J. L.; Thémans, B.; Fripiat, J. G.; André, J. M.; Chance, R. R. *Phys. Rev. B* **1984**, *29*, 6761.
(8) Nayak, K.; Marynick, D. S. *Macromoledules* **1990**, *23*, 2237.
(9) Karpfen, A.; Kertesz, M. *J. Phys. Chem.* **1991**, *95*, 7680.
(10) Kürti, J.; Surján, P. R. *J. Chem. Phys.* **1990**, *92*, 3247.
(11) Lazzaroni, R.; Riga, J.; Verbist, J. J.; Brédas, J. L.; Wudl, F. *J. Chem. Phys.* **1988**, *88*, 4257.
(12) Wallnöfer, W.; Faulques, E.; Kuzmany, H. *J. Chem. Phys.* **1989**, *90*, 7585.
(13) Wallnöfer, W.; Faulques, E.; Kuzmany, H.; Eichinger, K. *Synth. Met.* **1989**, *28*, C533.
(14) Hoogmartens, I.; Vanderzande, D.; Martens, H.; Gelan, J. *Synth. Met.* **1991**, *41*, 513.
(15) Schaefer, J.; Stejskal, E. O.; Buchdahl, R. *Macromolecules* **1975**, *8*, 291.
(16) Pines, A.; Gibby, M. G.; Waugh, J. S. *J. Chem. Phys.* **1973**, *59*, 569.
(17) Hartmann, S. R.; Hahn, E. L. *Phys. Rev.* **1962**, *128*, 2042.
(18) Lowe, I. J. *Phys. Rev. Lett.* **1959**, *2*, 285.
(19) Yannoni, C. S. *Acc. Chem. Res.* **1982**, *15*, 201.
(20) Opella, S. J.; Frey, M. H. *J. Am. Chem. Soc.* **1979**, *101*, 5854.
(21) Zumbulyadis, H. *J. Chem. Phys.* **1987**, *86*, 1162.
(22) Kiaoling, W.; Shanmin, Z.; Xuewen, W. *J. Magn. Reson.* **1988**, *77*, 343.
(23) Dewar, M. J. S.; Zoebisch, E. J.; Healy, E. F.; Stewart, J. J. P. *J. Am. Chem. Soc.* **1985**, *107*, 3902.
(24) Karpfen, A.; Ladik, J.; Russeger, R.; Schuster, P.; Suhai, S. *Theor, Chim. Acta* **1974**, *34*, 115.
(25) Ciolowski, J. *Chem. Phys. Lett.* **1988**, *153*, 446.
(26) Cui, C. X.; Kertesz, M.; Jiang, Y. *J. Phys. Chem.* **1990**, *94*, 5172.
(27) Brédas, J. L.; Chance, R. R.; Silbey, R.; Nicolas, G.; Durand, Ph. *J. Chem. Phys.* **1981**, *75*, 255.
(28) Brédas, J. L.; Chance, R. R.; Silbey, R.; Nicolas, G.; Durand, Ph. *J. Chem. Phys.* **1982**, *77*, 371.
(29) Wu, C. R.; Nilsson, J. O.; Inganäs, O.; Salaneck, W. R.; Österholm, J. E.; Brédas, J. L. *Synth. Met.* **1987**, *21*, 197.
(30) Orti, E.; Stafström, S.; Brédas, J. L. *Chem. Phys. Lett.* **1989**, *164*, 240.
(31) Lazzaroni, R.; Sato, N.; Salaneck, W. R.; dos Santos, M. C.; Brédas, J. L.; Tooze, R. P.; Clark, D. T. *Chem. Phys. Lett.* **1990**, *175*, 175.
(32) Van Bolhuis, F.; Wynberg, H.; Havinga, E. E.; Mejer, E. W.; Staring, E. G. J. *Synth. Met.* **1989**, *30*, 381.
(33) Hotta, S.; Waragai, K. *J. Mater. Chem.* **1991**, *1*, 835.
(34) Reynolds, J. R.; Ruiz, J. P.; Child, A. D.; Nayak, K.; Marynick, D. S. *Macromolecules* **1991**, *24*, 678.
(35) Barton, T. J.; Kippenhan, R. C. *J. Org. Chem.* **1972**, *37*, 4194.
(36) Cava, M. P.; Mitchell, M. J.; Deana, A. *J. Org. Chem.* **1960**, *25*, 1481.
(37) Jen, K. Y.; Elsenbaumer, R. *Synth. Met.* **1986**, *16*, 379.
(38) Hoogmartens, I.; Vanderzande, D.; Martens, H.; Gelan, J. *Synth. Met.* **1992**, *47*, 367.
(39) Nouwen, J. Ph.D. Thesis, Limburg University, 1992.
(40) Kreher, R. P.; Kalischko, J. *Chem. Ber.* **1991**, *124*, 645.
(41) Omran, S. M. A. R.; Harb, N. S. *J. Prak. Chem.* **1973**, *315*, 353.
(42) Chasar, D. W.; Pratt, T. M. *Synthesis* **1976**, *262*.
(43) Cohen, Y.; Klein, J.; Rabinovitz, M. *J. Chem. Soc., Chem. Commun.* **1987**, 1538.
(44) Volz, W.; Voss, J. *Synthesis* **1990**, 670.
(45) Dupuis, M. private communication.
(46) Lee, Y. S.; Kertesz, M. *Int. J. Quantum. Chem., Quantum Chem. Symp.* **1987**, *21*, 163.
(47) Mintmire, J. W.; White, C. T.; Elert, M. L. *Synth. Met.* **1987**, *16*, 235.
(48) Kobayashi, M.; Colaneri, N.; Boysel, M.; Wudl, F.; Heeger, A. J. *J. Chem. Phys.* **1985**, *82*, 5717. Dale, S. M.; Glidle, A.; Hillman, A. R. *J. Mater. Chem.* **1992**, *2*, 99.
(49) Whangbo, M. H.; Hoffman, R.; Woodward, R. B. *Proc. R. Soc. London Ser. A* **1979**, *366*, 23.
(50) Chung, T. C.; Kaufman, J. H.; Heeger, A. J.; Wudl, F. *Phys. Rev. B* **1984**, *380*, 702.
(51) Tsai, E. W.; Basak, S.; Ruiz, J. P.; Reynolds, J. R.; Rajehswar, K. *J. Electrochem. Soc.* **1989**, *136*, 3683.
(52) Okuda, Y.; Lakshnikansthan, M. V.; Cava, M. P. *J. Org. Chem.* **1991**, *56*, 6024.

Registry No. 1 (homopolymer), 117116-78-6; 1 (dimer), 144692-61-5; 1 (trimer), 144692-62-6; 1 (tetramer), 144692-63-7; 1 (hexamer), 144692-64-8; 2, 3533-72-0; 6, 144692-60-4; A1, 270-82-6; A2, 16587-39-6; Q1, 36740-03-1; Q2, 42314-33-0; PhCHO, 100-52-7; 2-chloro-1,3,2-benzodioxaphosphole, 1641-40-3.